Tectonic and climatic controls on Quaternary fluvial processes and river terrace formation in a Mediterranean setting, the Göksu River, southern Turkey

Nurcan Avşin[a]*, Jef Vandenberghe[b], Ronald van Balen[c], Nafiye Güneç Kıyak[d], Tuğba Öztürk[e]

[a]Department of Geography, Yüzüncü Yıl University, 65000 Van, Turkey
[b]Faculty of Earth and Life Sciences, Vrije Universiteit, De Boelelaan 1085, 1081 HV Amsterdam, The Netherlands
[c]TNO–Geological Survey of the Netherlands, 2595 Utrecht, The Netherlands
[d]Department of Energy Systems Engineering, Faculty of Engineering and Architecture, Beykent University, 34398 Istanbul, Turkey
[e]Department of Physics, Faculty of Science and Arts, Isik University, 34980 Istanbul, Turkey
*Corresponding author e-mail address: nurcanavsin@yahoo.com

Abstract

Climate and tectonics effect the fluvial evolution of the Mediterranean Mut basin. The basin contains a river terrace staircase of 16 levels (T16–T1) ranging from 365 to 10 m above the current Göksu River in its middle and lower sections. These river terraces records tectonic uplift in the Mut basin. Optically stimulated luminescence (OSL) dating of the fluvial sediments of the youngest terrace (T16) provides a chronology for the assessment of the important impacts of climatic changes. The ages from the youngest river terrace deposits in T16 may be subdivided into two intervals: (1) 239–194.7 ka during the later part of Marine Oxygen Isotope Stage (MIS) 7, implying that the aggradation of T16 started in (the final phase of) this warm period; and (2) 187.9–171 ka during much of MIS 6. Thus, it appears that the Göksu River continued depositing sediment from an interglacial into a glacial time. The differences in climate-driven fluvial evolution between this Mediterranean fluvial system and the classical, well-studied temperate–periglacial river systems in Europe may be the result of different vegetation cover and greater thaw of more intense snowfalls.

Keywords: River terrace; Fluvial aggradation; OSL dating; Climate control; Göksu River; Turkey

INTRODUCTION

River terraces are key elements for understanding fluvial landscape evolution. The general view is that they have formed as a result of climatic changes in combination with tectonic uplift (e.g., Schumm, 1977; Vandenberghe, 1995; Bridgland, 2000; Tebbens and Veldkamp, 2001; Vandenberghe and Maddy, 2001 Starkel, 2003; Peters and Van Balen, 2007; Starkel et al., 2015; Wang et al., 2015). Climate influences fluvial systems through variations in temperature and precipitation that cause further changes in vegetation, sediment supply, and river discharge (e.g., Vandenberghe, 1993, 2002; Bridgland, 2000; Stange et al., 2013). According to Penck and Bruckner (1909), aggradational terraces in upper zones of catchments are products of glacier ice thaw and its outwash. Similarly, Büdel (1977) suggested that cold-period braided rivers have extensive terrace bodies due to high sediment supply, whereas warm-period meandering rivers are characterized by incision. More recently, terrace sequences have been considered as representing climatic cyclicity in combination with tectonic uplift, with fluvial activity concentrated at cold–warm transitions (Vandenberghe, 1995, 2015; Bridgland, 2000; Vandenberghe et al., 2011). In addition, the response of rivers to climatic change is considered to be nonlinear and characterized by unequal preservation chances (Vandenberghe, 1993, 1995, 2015).

Bridgland and Allen (1996) proposed a climate-driven terrace-formation model to evaluate the impact of relatively stable conditions (glaciations and interglaciations) and unstable climatic transitions that are linked to terrace-forming incision. Maddy et al. (2001) applied and adopted the latter model in their study of the terrace sequence of the Thames Valley in England. In these models, a minor incision phase during warm–cold transitions and a phase of major incision at the warming limb of glacial–interglacial transitions were distinguished. Finally, Vandenberghe (2015) suggested

three main scenarios of depositional-erosive development in climate-driven river terrace staircases in accordance with the preservation chances of that development. To conclude, both glacial and interglacial periods may appear as relatively stable phases, with reduced fluvial morphological activity with a nival discharge regime during glaciations, and precipitation-driven discharge and single-channel river morphology during interglaciations (Maddy et al., 2001; Vandenberghe, 2008; Stange et al., 2013). Toward the termination of glacial times, fluvial aggradation intensified, especially in regions where glacial meltwater discharges and sediment supply significantly increased (Cordier et al., 2012; Stange et al., 2013).

However, some studies report a different temporal framework for the aggradation–incision phases in river valleys, ascribing aggradation to interglaciations, for example, Olszak (2011), Doğan (2011), Stange et al. (2013), Schielein et al. (2015), Olszak and Adamiec (2016). For instance, the river terrace deposits date to Marine Oxygen Isotope Stages (MIS) 7 and 5 in the Pyrenees foreland and are explained as being caused by aggradation related to minor cold periods (stades) within interglaciations (Stange et al., 2013), whereas in the west Carpathians, the terrace accumulations date to MIS 5 and 3 and are explained as being caused by aggradation related to interstades or interglaciations comparable with the those of Holocene (Olszak and Adamiec., 2016). Another investigation within the northern Alpine foreland has recognized different gravel units within one terrace, reflecting terrace aggradation during both MIS 7 and 6, separated by a sharp boundary between the two gravel units (Schielein et al., 2015).

This paper aims to evaluate the youngest river terrace level of the Göksu River in Anatolia of eastern Turkey, using morphological and sedimentologic analyses and optically stimulated luminescence (OSL) dating to help examine fluvial changes during relatively warm and cold cycles in a Mediterranean setting. We demonstrate that the fluvial evolution of the Göksu River seems to be quite different from fluvial evolution in standard temperate environments and might be typical for Mediterranean settings.

The long-term incision of the Göksu River basin was studied using river terraces by Schildgen et al. (2012). Their results are based on TCN-dated terrace levels, higher than ours, and an age estimate of the upper (marine) surface. They concluded a fast, long-term uplift rate of 0.25–0.37 mm/yr. Öğretmen et al. (2018) recently estimated a younger age of the upper surface, implying an even faster long-term uplift rate of 3.21–3.42 mm/yr. However, we show that for the last fluvial aggradation–incision phases, the short-term uplift rate likely has been slower, at about 0.05 mm/yr.

STUDY AREA

The Anatolian plateau is an integral part of the western reaches of the Alpine–Himalayan orogenic belt (Fig. 1), which formed during the Cenozoic by accretion of different lithospheric plates as a result of closure and suturing of the northern and southern branches of the Neotethys Ocean

(Şengör and Yılmaz 1981; Görür et al., 1984; Schildgen et al., 2012). In particular, the central and eastern Anatolian plateaus represent the westernmost boundary of the largest continental collision belt on Earth, extending from the Turkish–Iranian–Caucasus orogen to the Himalayan–Tibetan orogen and resulting from the collision of Arabia and India with Eurasia (Schildgen et al., 2012). The Anatolian plateau consists of oceanic and continental units shortened in the late Cretaceous–Eocene during the closure of the Mesozoic Neotethys Ocean and subsequent collision between the Taurus carbonate platforms and the crystalline complex of central Anatolia (Şengör and Yılmaz, 1981; Schildgen et al., 2012).

A number of fluvial surveys in Turkey have aimed to determine the timing of fluvial landscape evolution and its relationship with changing tectonic activities, internal dynamics, and climatic fluctuations. These surveys revealed that several rivers in Turkey have been affected by climatic changes as well as by tectonic movements (Westaway et al., 2004, 2006; Maddy et al., 2005, 2008; Doğan, 2010, 2011; Avşin, 2011; Demir et al., 2012; Bridgland et al., 2017). By dating Kizilirmak River terraces in central Anatolia, Doğan (2010, 2011) also found that fluvial deposition occurred in the warm periods and incision in the cold periods, which is contrary to the earlier models of climate-induced nonlinear river activity. The central Anatolian results, based on Ar-Ar dating of a basalt sequence capping the youngest river terrace, river terrace stratigraphy, and paleosol records in Anatolia, show that the coldest periods were not always characterized by aggradation of the fluvial systems.

The Göksu River in the Neogene Mut basin (Akarsu, 1960; Gedik et al., 1979; Tanar, 1989; Eriş et al., 2005; Bassant et al. 2005; Schildgen et al., 2012) is located in the Taurus Mountains' tectonic zone at the southern margins of the central Anatolian plateau and has its source in the central Taurus Mountains, flowing to the Mediterranean Sea across the Silifke delta and draining an area of ~10,400 km^2 (Fig. 1). A well-developed terrace sequence is present along the Göksu River. The study area, located between the Derincay Gorge and Silifke, includes the middle and lower sections of the Göksu River valley (Fig. 1). The Göksu River has developed its course on late Miocene marine sediments of the Mut and Koselerli Formations. Previous fluvial morphological studies reported multiple terrace levels and concluded that the river has been affected by tectonism, climatic change, and sea-level change (Çiçek, 2001; Schildgen et al., 2012).

METHODS

Field Data Collection

Fieldwork included mapping of river terraces, characterizing sedimentary sequences, and sampling for OSL dating. To establish the extent of the preserved river terraces, detailed geomorphic mapping was carried out aided by 1:25,000 topographic and geologic maps. (MTA, 1996; HGK, 2000) Elevations of river terrace levels above the present-day riverbed
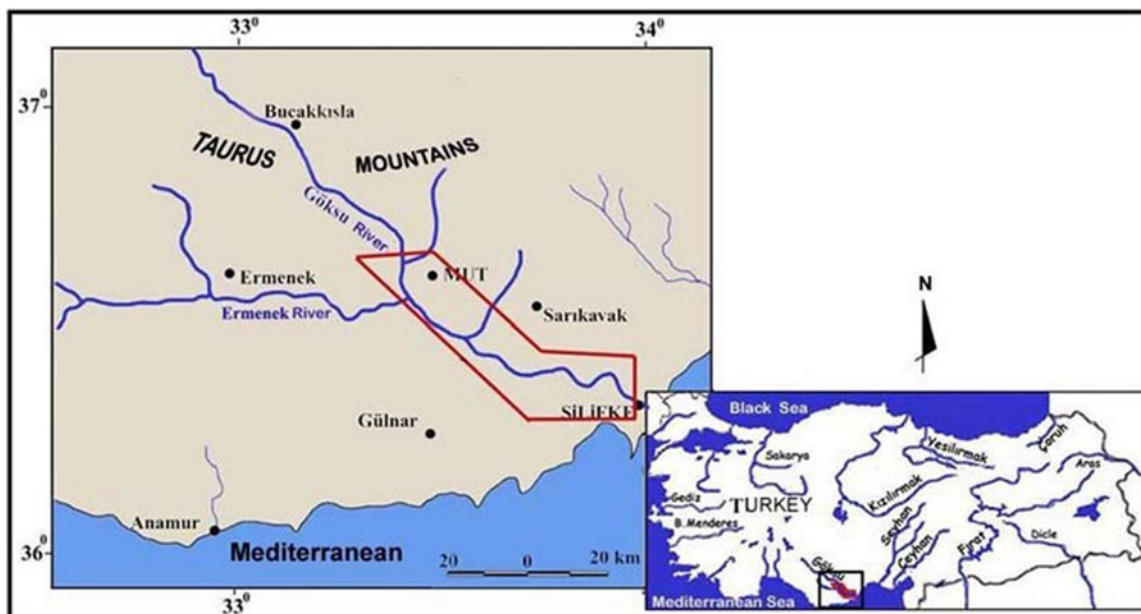
Figure 1. (Color online) Location map of the study area.

were measured using a barometric device in a handheld GPS with a standard error of 1 m. These elevations were measured at the bedrock contact in the majority of cases and were estimated in a very few cases. River terrace elevations were measured at the base of fluvial deposits, where present. Suitable sand samples for OSL dating were present only in the youngest river terrace. Therefore, 10 samples of the terrace sediments were collected for quartz OSL dating in two separate parts of the same terrace level. Sedimentary interpretations are mainly based on detailed archiving and analysis of the sedimentary structures observed in a number of exposures. The sediments were described according to Miall's (1996) lithofacies classification/codes, lithologic properties, and thickness to reconstruct likely sedimentary processes. Reconstructions of fluvial architecture were difficult because of the lack of 3D sections. In addition, the current bed pattern was assessed on the basis of Schumm's classification (Schumm, 1977, 1981), which is based on the degree of meandering–braiding of individual channel beds.

OSL dating

Sediment samples were collected in opaque metal tubes from various depths around Köselerli village (Fig. 2C). Luminescence analyses were prepared and conducted at the Luminescence Research and Archeometry Laboratory in Istanbul under dimmed red light. The sediment was sieved to separate grains of 90–180 μm size. The quartz grains were extracted from the bulk sediment using 10% HCl and 10% H_2O_2 for the removal of carbonates and organics, respectively. HF treatment enabled the quartz grains to be etched to clean the outer surface from alpha particles and was followed by one more HCl treatment, washing with distilled water, and drying in an oven at 50°C.

Each sample was divided into 16 aliquots. The quartz grains of each aliquot were checked for feldspar contamination using infrared stimulation and were also subjected to other reliability tests described below (Fig. 3). The measurements were performed with an automated Risø TL/OSL reader (model TL/OSL-DA-15) equipped with an internal $^{90}Sr/^{90}Y$ beta source (~0.1 Gy/s), blue light-emitting diodes (LEDs) (470 nm, ~40 mW/cm^2), and infrared LEDs (880 nm, ~135 mW/cm^2). Luminescence signals were detected using an EMI 9635QA photomultiplier tube fitted with 7.5-mm-thick Hoya U-340 filters (Bøtter-Jensen, 1997). The equivalent dose (D_e, measured in Gy) was estimated using the single-aliquot regeneration dose method (SAR) developed by Murray and Wintle (2000).

The concentrations of radioactive isotopes uranium, thorium, and potassium were measured by ICP-ES/ICP-MS analysis at Acme Analytical Laboratories (Vancouver) in Canada. The alpha contribution to dose rate was eliminated due to the etching of quartz grains with HF treatment. The cosmic contribution to the dose rate was obtained using the known latitude, longitude, and elevation of the site and the burial depth of each sample (Prescott and Hutton, 1988). Radioactive content, cosmic contribution to dose rates, and obtained dose-rate values were between 0.40 and 0.78 Gy/ka. The moisture content was estimated from present-day values. Full details of dose-rate determination, equivalent dose, and age estimates are shown in Table 1.

The SAR protocol of Murray and Wintle (2000) used in this study has six cycles: natural dose, three regeneration doses, zero dose, and then repetition of the first regeneration dose. In each cycle, the aliquot was preheated at 260°C for 10 s to remove unstable elements of the signal; this was followed by OSL measurement (L_i), recorded under blue light stimulation at 125°C for 40 s. A constant test dose, T_D, was
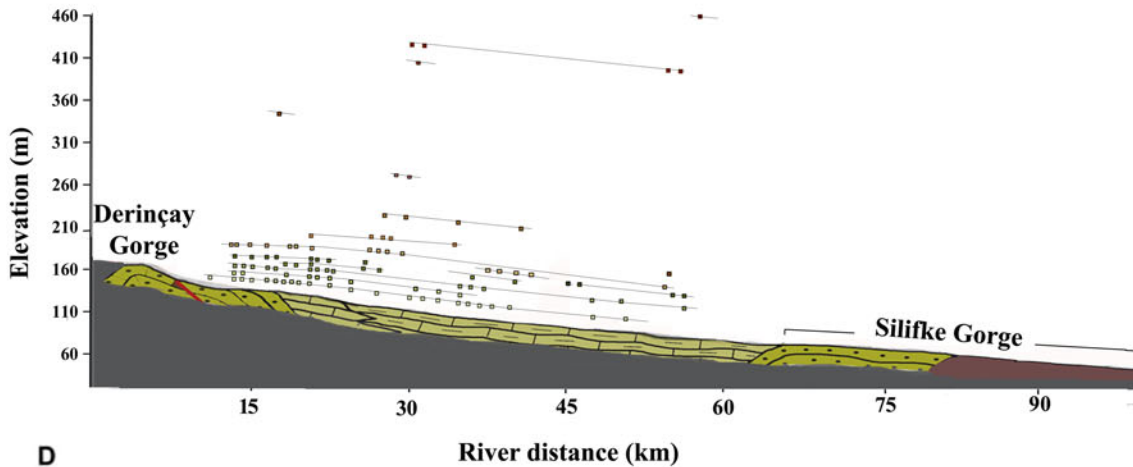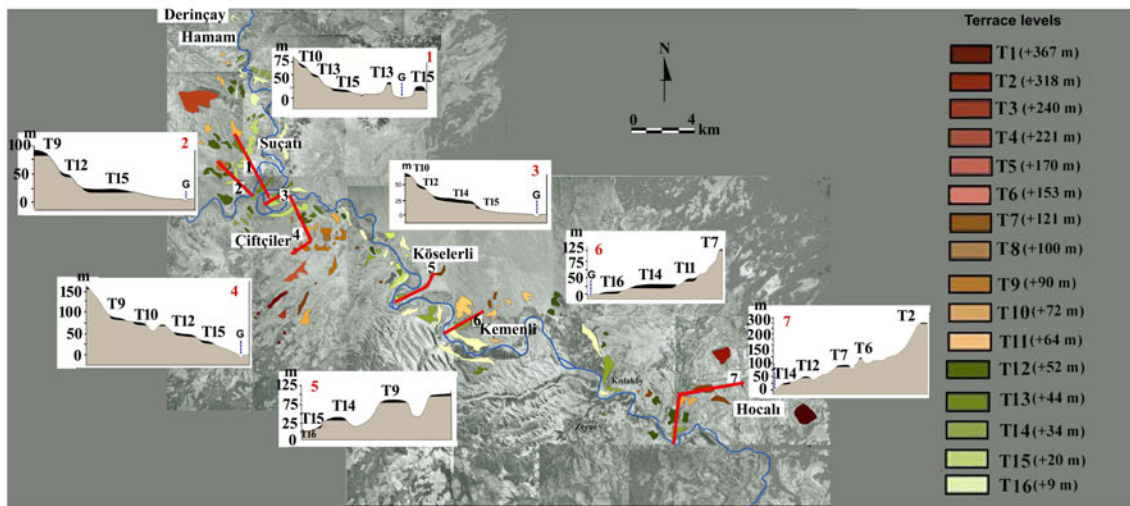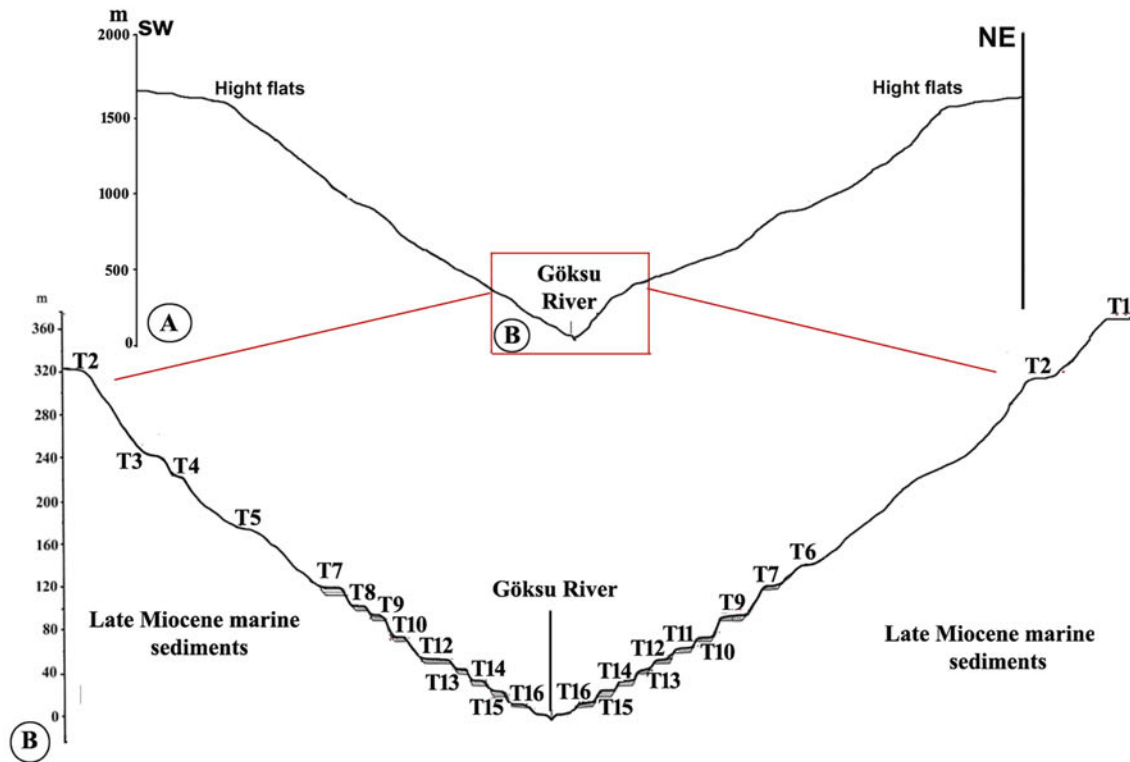
Figure 2. (Color online) (A and B) The generalized section of the Göksu River valley. The elevations are basement levels of the river terraces. (C) River terrace distribution in the middle and lower parts of the Göksu River valley. The cross sections and red lines (1–7) show the levels of river terraces. (D) Longitudinal profile and terraces of the Göksu River.
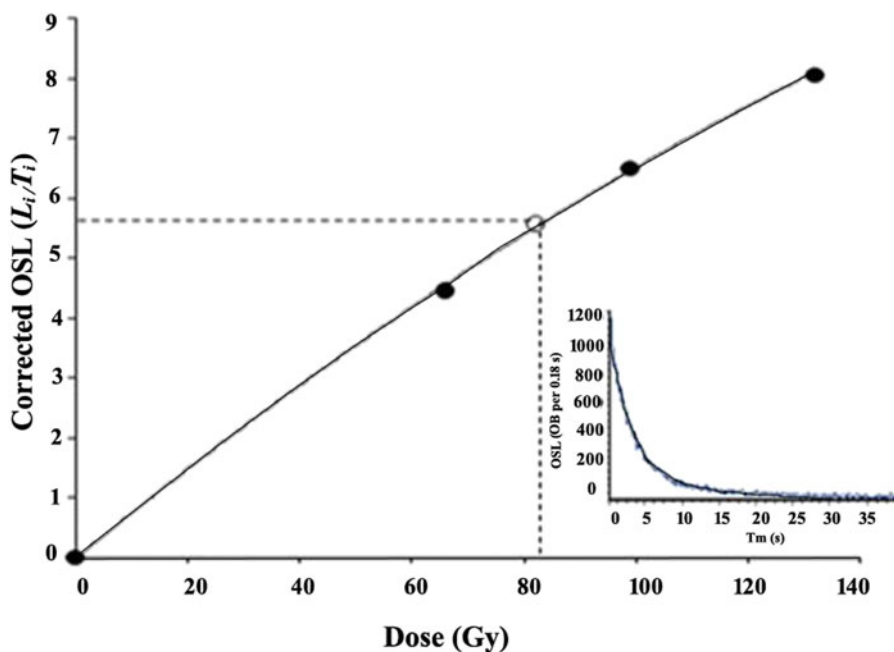
Figure 3. (Color online) Dose-response and shine-down curves (the latter is inset) for a representative aliquot from sample GP-05.

administered to the same aliquot, and the luminescence signal was recorded (T_i) to monitor and correct for sensitivity change (L_i/T_i). Then, a dose–response curve was constructed using the corrected regenerative signals as depicted in Fig. 2 for a representative sample (GP-05), for which the equivalent dose D_e was obtained as 90.7 Gy from the interpolation of the corrected natural signal on the dose–response curve. The final equivalent dose (D_e) used for age estimation calculation is the arithmetic mean of all equivalent doses obtained on accepted aliquots for each sample. Aliquots were accepted (68%–88% acceptance rate) when they had recycling ratios within 10% of unity (where the first regeneration dose was administered once more to the same aliquot to determine the repeatability of the same dose point on the dose–response curve) and low recuperation. Reliability was also checked through a dose-recovery test on sample GP-08, which yielded a value close to 1, suggesting that the protocol was suitable for use

on these samples (Olley et al., 1996; Murray and Wintle2003).

RESULTS

General terrace morphology

The remnants of horizontal surfaces along the Göksu River (T1–T16) at ∼50–100 km inland from the Mediterranean Sea occur at a wide range of altitudes ranging from between 10 to 367 m above the present-day river channel (Fig. 2C, Table 2). The lower levels, considered river terraces (T16–T12), are preserved throughout the valley.

No terraces were present in the Derincay and Silifke gorges, located north and south of the area, respectively. Between the two gorges, fragments of the higher levels, T1–T6, are present only at a few localities, making the

Table 1. Details of equivalent dose (D_e), concentrations of radioactive elements and age estimates for samples GP-01 to GP-10.[a]

Laboratory number	Depth (m)	OSL age (ka, ± σ)	D_e (Gy)	No. of aliquots	Dose rate (Gy/ka)	Cosmic (Gy/ka)	Moisture content %	U (ppm)	Th (ppm)	K (%)
GP-01	0.52	115.5 ± 8.8	90.65 ± 5.71	13	0.78 ± 0.03	0.11	24.9	3.1	0.8	0.06
GP-02	0.48	187.9 ± 20.4	87.09 ± 7.14	14	0.46 ± 0.03	0.12	24.95	1.2	0.9	0.09
GP-03	0.40	239.0 ± 23.2	96.20 ± 4.93	12	0.40 ± 0.03	0.14	25.00	1.0	0.5	0.07
GP-04	0.30	187.9 ± 15.1	97.58 ± 4.66	12	0.52 ± 0.03	0.15	24.92	1.5	0.9	0.08
GP-05	0.47	177.0 ± 14.2	102.38 ± 5.74	13	0.58 ± 0.03	0.12	25.05	1.7	1.0	0.11
GP-06	0.33	199.0 ± 14.8	102.88 ± 3.80	12	0.52 ± 0.03	0.15	25.10	1.5	0.6	0.07
GP-07	0.35	171.0 ± 13.3	88.33 ± 5.01	12	0.52 ± 0.03	0.18	52.90	1.8	0.7	0.07
GP-08	0.16	200.9 ± 16.2	91.59 ± 2.91	11	0.46 ± 0.00	0.18	24.94	0.9	0.7	0.09
GP-09	0.15	194.7 ± 17.7	93.51 ± 5.36	12	0.48 ± 0.03	0.18	24.98	1.0	0.9	0.08
GP-10	0.15	197.9 ± 19.9	97.20 ± 3.55	12	0.49 ± 0.05	0.19	24.85	0.9	1.1	0.09

[a]The equivalent dose used is the arithmetic mean of all equivalent doses obtained from accepted aliquots for each sample.

Table 2. Altitudes of river terrace bases and thicknesses of river terrace deposits.

Terrace code	T16	T15	T14	T13	T12	T11	T10	T9	T8	T7	T6	T5	T4	T3	T2	T1
Elevation of terrace base (m)	9–12	20–22	30	44	52	64	72–75	90–92	100	120–122	153	170	221	240	318	367
Thickness (m)	7–8	3–4	4–5	4–5	4–5	2	2–3	6–7	2	2–4	0	0	0	0	0	0

correlation of these fragments problematic. The correlation of the other river terraces along the river is straightforward according to the field mapping. River terraces, particularly in the middle part of the valley, form a staircase of river terrace features, each overlying a significant thickness of sediments assigned to T7–T16 (Fig. 2A and B, Table 1). The elevations and slopes (longitudinal gradients) of the terraces decrease gradually and regularly in the downstream direction (Fig. 2D).

Morphology and sedimentology of the fluvial deposits

Higher levels (T1–T6)

The flat surfaces T1–T6 range from 153 to 367 m above the present-day river channel and have been eroded into late Miocene marine sediments. At a few localities, for example, at the entrance of the Silifke Gorge around Hocalar and at the junction point of the Ermenek and Göksu Rivers around Çiftçiler, some of these higher levels, in particular T1 and T2, are covered with boulders to fine-grained pebbles, and stratification is absent (Fig. 2A–C). The clasts are mostly angular or semi-angular and entirely composed of limestone and are considered to be in situ weathering products that were probably reworked by slope processes. The surfaces T1–T6 rarely contain fluvial deposits and are limited in extent. Therefore, we indicate the surfaces as "levels," not "terraces."

Lower and medium terraces (T7–T15)

In comparison with the higher levels (T1–T6), the younger river terraces are relatively well preserved and expose lithified conglomerate deposits with thicknesses between 1 and 10 m. Deposits from the different river terraces exhibit similar sedimentary characteristics along the entire investigated section of the valley. Covers of alluvial fan and slope sediments are only rarely present on the tops of river terraces. The elevations of the lower and medium terraces range from 10 to 121 m above the present-day river channel.

Terrace 7 (T7) is the highest terrace with exposed fluvial deposits, and it occurs at both sides of the valley at several locations. The gravel units have imbricated, well-rounded pebbles that are well cemented and unsorted, with grain size varying from coarse to fine gravel with diameters of 2 to 6 cm. The gravels occur in crudely bedded (Gh facies of Miall [1996]), horizontally (Gh) and incised stratified layers (Gp). Terrace 8 (T8), which only occurs at one point near Çiftçiler, is composed of well-rounded and cemented, clast-supported, crudely bedded conglomerates (Gh), which have a thickness of 2 m.

Terrace 9 (T9) is one of the most extensive of the middle river terraces and appears at several locations in the valley. In general, the deposits of this level consist of well-cemented, inclined (Gp) or tabular sets of cross-bedded and crude horizontally stratified conglomerates (Gh) with coarse, clast-supported, well-rounded gravels, interpreted as transverse and longitudinal bed forms, as in T8. The deposits that compose T9 around Çiftçiler display in the upper part of the section around that village, crude, horizontally laminated, fine sediments (Fl) that overlie the sandy gravel layers. Between these fine sediments, gravels occur in minor channel fills (Gt).

Terrace 10 (T10) occurs at several points, for example, south of the Derincay Gorge, (between Hamam and Çiftçiler villages) and at the entrance of the Silifke Gorge, near Hocalar village. Locally, this level was observed together with lower and higher levels displaying a step-shaped morphology. Generally, the deposits closely resemble the T7 and T8 deposits. T11 is situated at only a few localities near Kemenli. T11 might be equivalent to T12, because the two terraces never occur at the same place. Terrace 12 (T12) is present at several localities, and the gravel deposits of T12 are similar to those at higher elevations and also reflect transverse bed forms.

Terrace 13 (T13) is one of the rarest terraces in the survey area. Terrace 14 (T14) is one of the most common lower levels, together with T15 and T16. This level has well-presented remnants that can be tracked almost uninterruptedly throughout the Göksu River valley. The terrace deposits are composed of cosets of inclined-stratified layers (Gp) and include mostly medium- to coarse-grained (1–6 cm diameter), unsorted, clast-supported, well-rounded gravels.

Terrace 15 (T15) occurs at several locations adjacent to T16, T13, and T12, displaying a staircase-like relief. The deposits of T15 around Çiftçiler and Hamam have similar internal structures, expressing the evolution of point bars and transverse bars. Heterogeneous grain size points to irregular discharge and unstable energy conditions. The deposits of this river terrace are similar to those in other terraces, especially in T14 and T16.

Youngest terrace (T16)

Terrace 16 (T16) is the most common and youngest river terrace within the valley. The deposit is much thicker (9–10 m) than those in other river terraces and exposes various sedimentary structures in the largest outcrop around Köselerli where all the OSL-dating samples were taken. Two lithofacies are present:

(1) Lithofacies 1, which occurs over a length of 0.3 km in different sections of T16, contains clast-supported, well-sorted, graded, crudely bedded (Gh), inclined-stratified (Gp), and trough-shaped cross-bedded (Gt) fine to coarse gravels (1–20 cm in diameter).

(2) Lithofacies 2 contains tabular sets of matrix-supported, inclined-stratified (Gp), and trough-shaped cross-bedded (Gt) relatively fine gravels and sands (Sl) or lens-shaped, horizontally laminated silt and clay (Fl, Fsm).

Lithofacies 1 suggests a gravelly river with sharp boundaries between the strata, mostly without fine-grained fills of abandoned channels but with longitudinal, transverse, or lateral bars (Fig. 4A–D). Lithofacies 2 is characterized by alternations of coarse-grained bedded deposits with different kinds of bars, finer-grained fills of depressions between the bars, and abandoned channels toward the top of T16 (Figs. 5A–C and 7A).

All sand samples for OSL dating were taken from homogeneous sand units. Samples 01–05 were collected from section T16a (Fig. 7). The sedimentary structure of sample 01 displays lens-shaped bedded, horizontally stratified, medium to coarse sand layers. These layers have a thickness of 35–40 cm. The sedimentary structure of samples 02 and 05 displays lens-shaped bedded, inclined-stratified, coarse sand layers. These layers have a thickness in of 25 cm. The deposit of sample 03 displays lens-shaped, grouped, planar-stratified, fine sand layers with a thickness of nearly 80 cm. Sample 04 occurs within trough-shaped, cross-bedded, fine sand layers with a thickness of nearly 1 m.

Samples 06–10 are located in section T16b (Fig. 7). Sample 06 was taken from within a trough-shaped, cross-bedded, fine sand layer some 40 cm thick. The deposit of sample 07 consists of lens-shaped bedded, inclined-stratified, medium and coarse sand layers. These layers have a thickness of 1.5 m. Sample 08 occurs in a lens-shaped bedded, horizontally stratified, coarse sand layer some 30–40 cm thick. The deposits of samples 09 and 10 consist of inclined-stratified, coarse sand layers. These layers have a thickness of 30–40 cm.

OSL ages

Ten sediment samples were collected from two localities with suitable quartz sand layers. These localities are in the central part of the valley, around Koselerli. The two deposits, 1.6 km apart, belong to the youngest terrace, T16 (Fig. 4B–D). Samples 01–05 were collected from T16a, the first part of T16 (36°32′50″N, 33°26′38″E), whereas samples 06–10 were collected from T16b, the second part of T16 (36°32′55″N, 33°26′39″E).

All the OSL ages presented are internally robust. Aliquot acceptance rates are high (68%–88%), dose-recovery testing of sample GP-08 was close to 1, and none of the samples are close to saturation. Figure 2 shows this clearly: interpolation of the natural signal has been undertaken on the linear part of the growth curve. This good luminescence behavior is probably linked to the very low dose rates (Table 1), meaning that older ages can be reliably obtained on quartz in this

river system more so than in some other settings. Shine-down curves show rapid loss of signal with time, suggesting dominance by the fast component (Fig. 2), and therefore less likelihood of partial bleaching. Most of the samples show normally distributed equivalent doses, with only two showing some negative skew (GP-02 and GP-07), both of which fall squarely within the range of most of the age estimates. For these reasons, we conclude there is no clear evidence of partial bleaching in these sediments (see Fig. 5) and the ages reported are robust. The two samples that fall outside this range are GP-01 (ca. 115 ka) and GP-03 (ca. 239 ka). Of these, sample GP-03 is less problematic, because its age range of 216–262 ka does overlap the combined age range of samples GP-08, GP-09, and GP-10 (ca. 200–195 ka) within uncertainty (Fig. 6, Table 1). Taking the uncertainty into account, it seems that the three lower samples of section 9B were deposited during MIS 7, while the other samples, occurring at a higher stratigraphic position, were deposited during MIS 6 (except GP-01).

The upper part of T16a is represented by one single age (GP-01: 115 ka). This does not overlap any other OSL ages, although it is at the highest elevation above the base of the terrace (Figs. 6 and 7) and thus in broadly stratigraphic order. One explanation for the younger age of GP-01 could be a higher dose rate, although its value of 0.78 (Table 1) is only slightly higher than other values around 0.5. Thus, provisionally, we favor instead the existence of a sedimentary hiatus between the sediment containing GP-01 and the sediments containing all the other samples, attributing the deposits containing GP-01 to a younger phase of fluvial activity than the older deposits. Such hiatuses between the OSL-dated sediments in a vertical section are not uncommon. An illustrative example is provided by von Suchodoletz et al. (2016), who demonstrate that older channel deposits are overlain by floodplain deposits from a considerably younger river that incised into those older channel deposits in the Kura River valley (southern Caucasus).

Despite the large uncertainties, and excluding sample GP-01, we suggest that deposition within this terrace body can be separated into two time periods. The first comprises samples GP-03, GP-08, GP-09, and GP-10 (Fig. 7) and can be broadly attributed to MIS 7–178 to 262 ka combined age range (Fig. 6). The second group comprises GP-02, GP-04, GP-05, GP-06, and GP-07, all of which occur at a higher elevation above the terrace base and can be attributed to deposition during MIS 6 (158 to 214 ka combined age range). The sediments deposited during MIS 7 and at lower elevation are characteristic of lithofacies 1, being mostly coarse sediment. In contrast, the altitudinally higher deposits deposited during MIS 6 comprise lithofacies 2 deposits, which are mixed sediments with finer gravels and more sand beds (Fig. 4). Thus, according to these ages, and taking into account the uncertainties, it seems that the fluvial aggradation started at the end of the MIS 7 warm period and continued into the MIS 6 cold period. After this, it seems likely there was an interval of nondeposition during the most climatically severe part of MIS 6, followed by reactivation of river
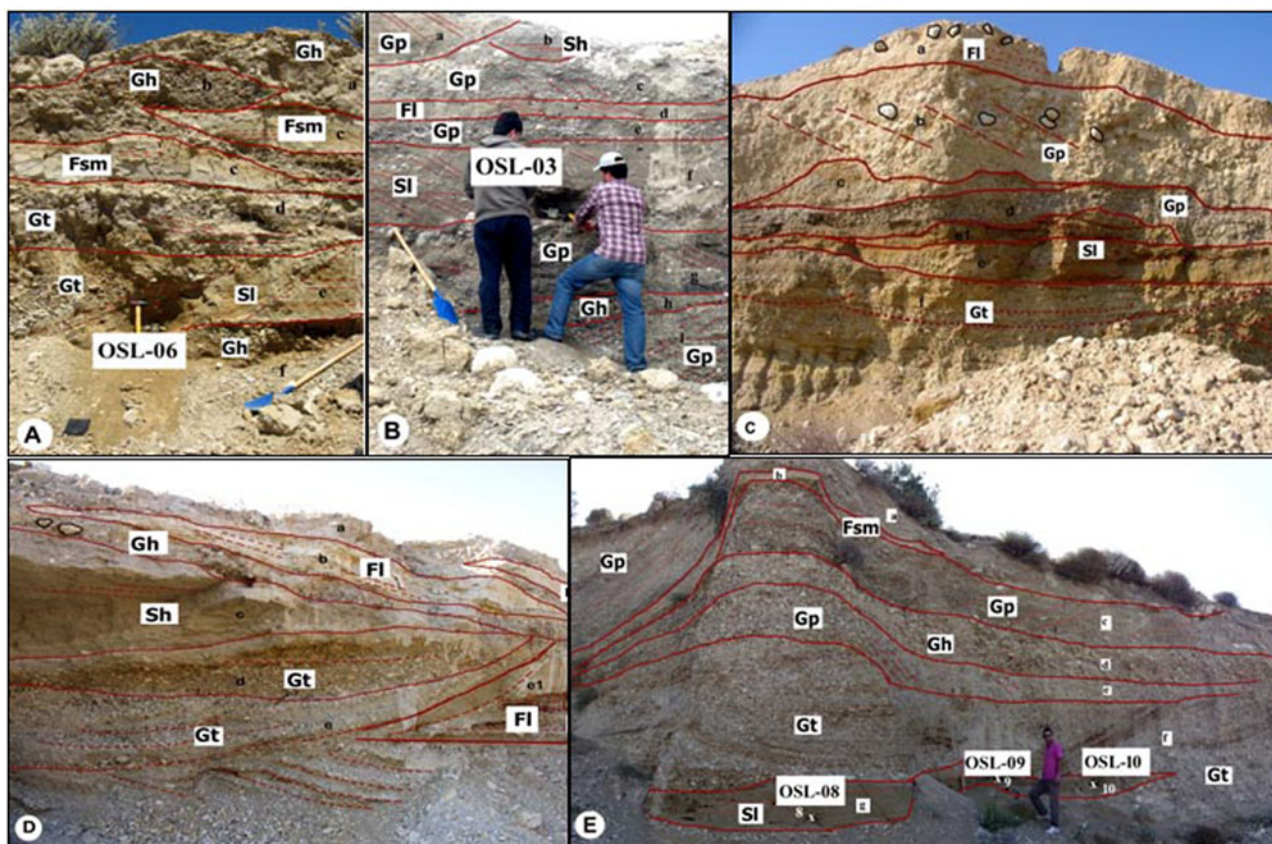
Figure 4. (Color online) Terrace 16 (9–10 m) and its sedimentologic character around Koselerli, displaying in A–C matrix-supported, low-angle inclined-stratified (B and C), sandy and relatively fine-grained gravels and inclined-laminated sands (lithofacies 2). Some parts display tabular sets of matrix-supported, inclined-stratified (Gp) and trough-shaped cross-bedded (Gt), relatively fine gravels and sands (Sl), or lens-shaped; horizontally laminated silt-clay (Fl, Fsm). Lens-shaped, crudely horizontally laminated silt-clay beds separate lithofacies 1 and 2. (D and E) illustrate lithofacies 1 with clast-supported, well-sorted, graded, crudely bedded (Gh), inclined-stratified (Gp), and trough-shaped cross-bedded (Gt), small to coarse gravels (diameter 1–20 cm).

activity during MIS 5, represented by sample GP-01. There is no clear evidence here for incision at the glacial–interglacial transition as suggested in the model of climatic forcing of river behavior outlined earlier (e.g., Maddy et al., 2001). Indeed, it is clear from these age estimates and the morphological relationships between the terrace deposits that no terrace-forming event occurred at this location either between MIS 7 and 6 or between MIS 6 and 5. It is possible, however, that after initial limited local reactivation of this river terrace surface in MIS 5 (represented by sample GP-01), a later terrace-forming incision occurred elsewhere in the valley.

DISCUSSION

Tectonic impact on valley development

Using biostratigraphic and paleomagnetic analyses, Schildgen et al. (2012) dated the uplifted and deeply incised marine Oligo-Miocene formations east of the Mut Basin (in the Başyayla section), located at an altitude of 2000 m, to 8 Ma, after which time the Göksu River started to incise due to subsequent uplift. According to the age of this uplift

(8 Ma) and the inferred ages (ca. 130–25 ka) and elevation (28–34 m) of one terrace elevation, Schildgen et al. (2012) calculated an average uplift rate of 0.25 to 0.37 mm/yr. That uplift rate deviates from the uplift rate we calculated (0.05 mm/yr), because our youngest terrace level was lower (9–12 m) and dated to an older age (ca. 262–218 ka, with an outlier of ca. 115 ka). Furthermore, the lowest terrace of Schildgen et al. (2012) is about 20 m higher than the lowest terrace in our study (T16). Öğretmen et al. (2018) recently estimated a younger age for the upper surface, implying an even faster long-term uplift rate (3.21–3.42 mm/yr). Finally, and according to our ideas put forward in the previous section, we have to stress that estimation of uplift rates based on the age of fluvial deposits of terraces must be made with caution. For instance, incision depth has to be based on the comparison of channel facies, not floodplain facies that may occur at higher elevations than the incised river bed. To conclude, it may be derived from the latter studies (including this study) that the uplift rate in the basin may have varied considerably during the Quaternary. In addition, tectonic fragmentation of the Anatolian region may have caused regionally different uplift rates.
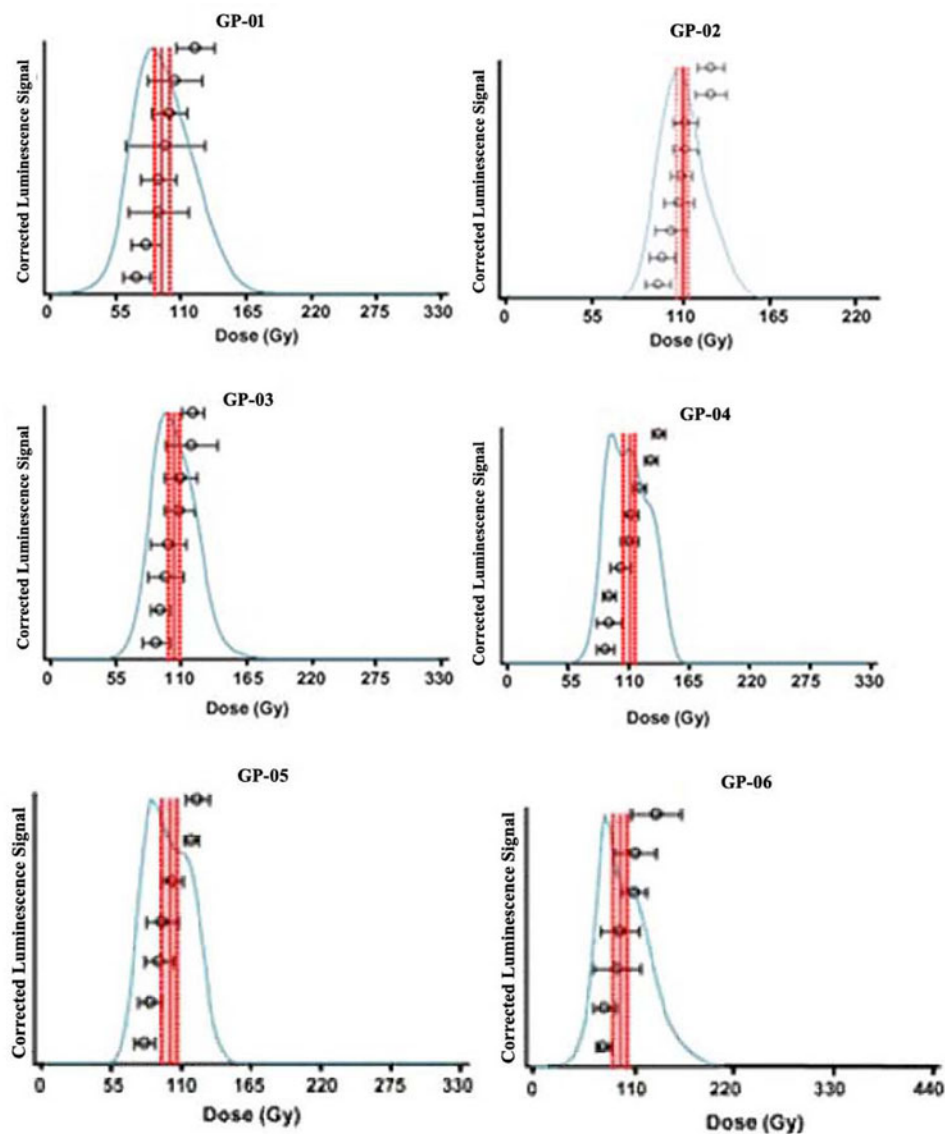
Figure 5. (Color online) Equivalent dose distributions for all samples GP01–GP10.

As concerns local faulting, it is not clear that faults affected the valley floor and the terrace levels throughout the Göksu River (Fig. 2D), but they caused an offset on the main river channel between Kemenli and Hocalı and steepening of the valley floors of the small tributary rivers that flow between Suçatı and Köselerli.

Comparison with the present-day river

The present-day (Holocene) Göksu River has gravel beds and is characterized by a low sinuosity and point bars or chute cut-off bars similar to the pre- Holosen river (Fig. 8). This wandering river type is intermediate between low-sinuosity, braided rivers with multiple channels and high-sinuosity meandering rivers with single channels (Miall, 1996; Makaske, 2001). The Holocene Göksu River contains mostly coarse-grained sediments within its point bars (Fig. 8) and

has low sinuosity (meandering degree of 1.2). The older Göksu River probably had a similar fluvial wandering pattern, especially during warm periods. Sedimentologic observations in the (lower) river terraces show that the river terrace deposits are dominated by varying cyclic coarse-gravel assemblages, from which we infer bar deposits, such as point bars, transverse bars, and longitudinal bars (Miall, 1996). Some channel-fill deposits are dominated by facies Gp, Gh, and Gt, with sand facies (Sl) and, on a limited scale, massive or finely laminated silt and clay (Fsm, Fl), comparable to the current river.

Drainage pattern reconstruction

While some river terraces (T8, T10, T11) have a sediment thickness of less than 4 m, all terrace deposits with sufficient thickness display similar sedimentary facies and facies
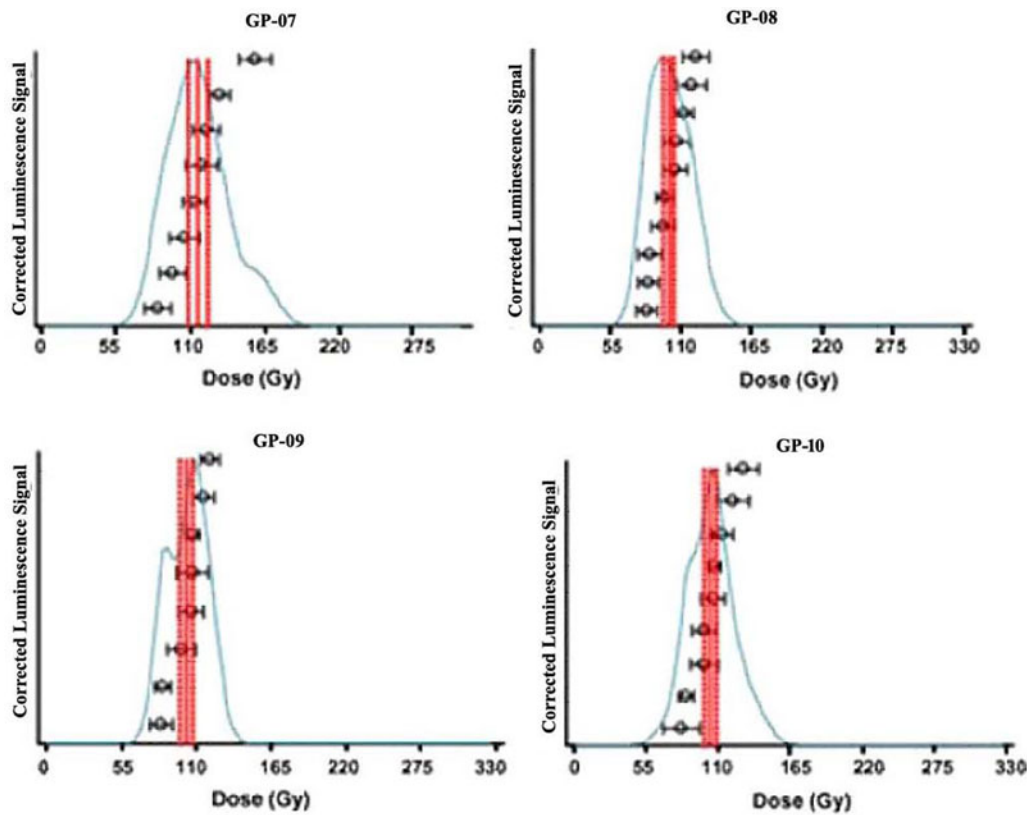
Figure 5. (Continued).

successions. In lithofacies 1, mostly clast-supported, well-sorted, well-rounded, inclined-stratified, crudely bedded, or trough-shaped stratified, coarse- to medium-grained gravels are dominant. Such deposits are preferentially located in the lower parts of the deposits, as is particularly well illustrated within the youngest terrace deposits (T16; Fig. 4A–D), which have a strong resemblance to the present-day river pattern of the Göksu River (see section 5.2:Comparison with the present-day river). Accordingly, lithofacies 1 is interpreted as a gravel-bed, wandering river (terminology by Church, 1983; Carson, 1984; Miall, 1996).

The second lithofacies (lithofacies 2) is represented by tabular sets of coarse- to fine-grained gravels with interbedded, lens-shaped, horizontally laminated sand, clay, and silt layers, also reflecting variable fluvial energy (Fig. 4A–C). These lens-shaped sets may have an internal, smaller-scale, inclined bedding than found in lithofacies 1. Because these layers are mostly located in the upper part of the deposits and are different from the lower lithofacies 1, a different phase of fluvial activity is interpreted. During this later phase, the river was still wandering as in the previous phase, but probably under lower energy conditions.

We suggest the following fluvial evolution model. While this is derived from the data in the youngest terrace (T16), we believe it to be valid for all Göksu terraces, because similar internal structures and successions were observed in them, although the overall thickness of sediment was much less. When the river started to aggrade in MIS 7 (GP-03,

GP-08, GP-09, GP-10), it was relatively energetic and accumulated coarse-grained gravel with migrating bars in a shallow single channel or channels, with clast-supported sediments (channel-fill deposits, Gt, Gp, and Gh, with sand facies, Sl: lithofacies 1). In the later phase of fluvial aggradation (MIS 6: GP-02, GP-04, GP-05, GP-06, GP-07), the energy decreased, and the river started to deposit relatively fine-grained sediments, including laminated sand, silt, and clay layers (channel-fill deposits, sandy overbank deposits, and fine-grained floodplain deposits: lithofacies 2). Sedimentary structures in the deposits from which the OSL samples were taken are interpreted as transverse bed forms, linguoid bed forms, and scour fills or humpback forms.

Role of climate

The present analysis of the climatic impact is valid for the entire series of terraces but is mainly based on the information from the youngest terrace (T16) and the present-day river morphology. T16 shows the most fully developed sediment series and is the only one dated. Assuming that the OSL ages are correct, apart from the youngest OSL age, which is considered an outlier, the ages of the river terrace deposits in T16 show an evolution starting from the later part of MIS 7. This implies that the aggradation of T16 started in a warm period or the final phase of a warm period. Its sedimentary facies (lithofacies 1) and drainage pattern also correspond with those of the present-day river. Later, the Göksu
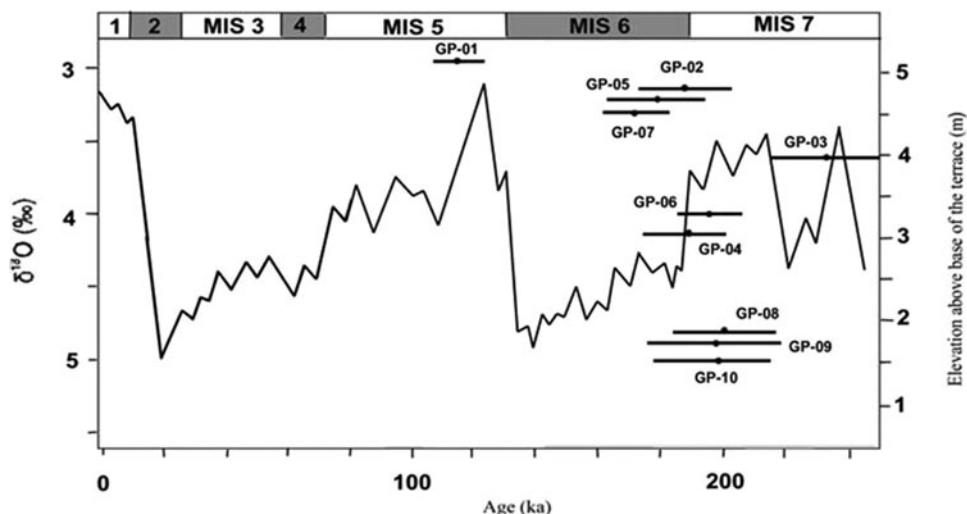
Figure 6. Distribution of the luminescence ages with error bars against Marine Isotope Stages after Cohen and Gibbard (2011), showing phases of aggradation since ca. 240 ka. These ages show that the fluvial aggradation started in the MIS 7 warm period and continued in the MIS 6 cold period.
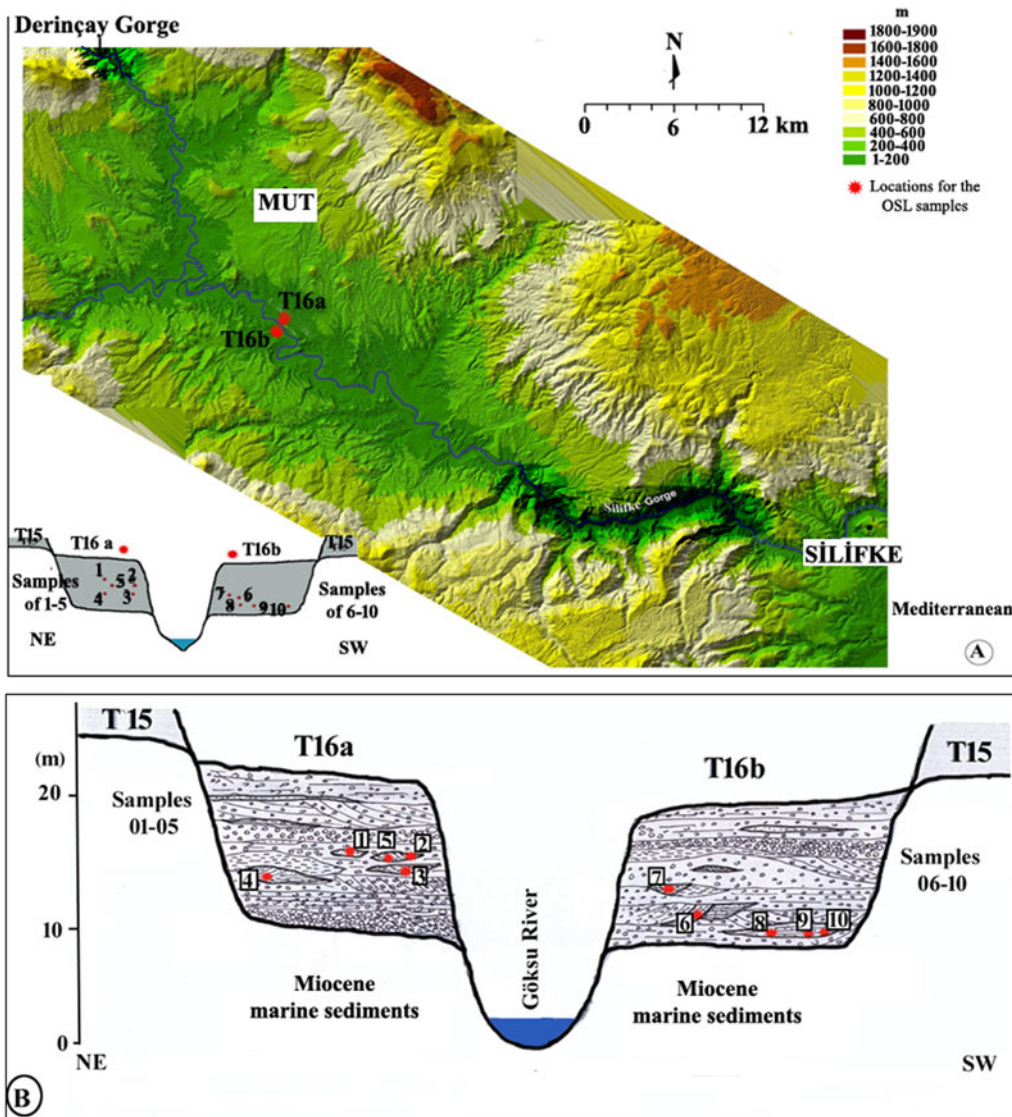

Figure 7. (Color online) (A and B) The OSL sample locations of T16a and T16b around Köselerli.
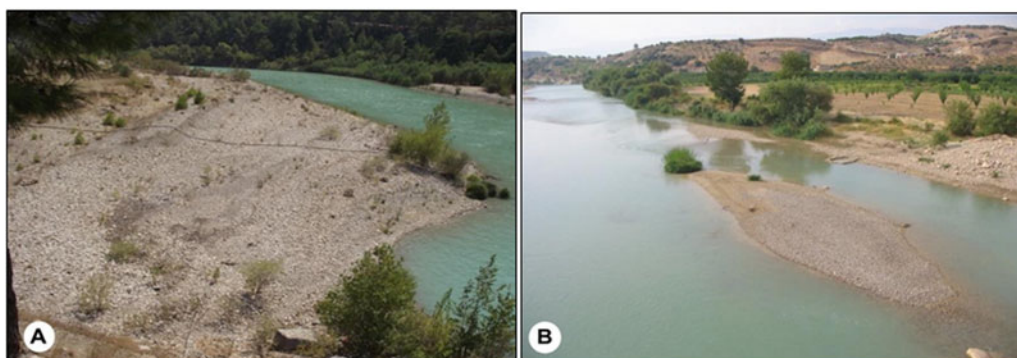
Figure 8. (Color online) Relatively coarse-grained sediment aggradation of the present-day (Holocene) river reflects a wandering gravel-bed river with longitudinal bar (B) and point bar (A).

River continued deposition during the MIS 6 cold period. The deposits have sedimentologic characteristics that are somewhat different from the previous ones, especially in their generally finer-grained texture (lithofacies 2). There is often an indistinct boundary between the two kinds of deposits.

A sedimentary succession similar to that of the Göksu River was reported from the northern Alpine foreland, where two different gravel units, separated by a sharp boundary, are superposed within one river terrace, reflecting terrace aggradation during both MIS 7 and 6 (Schielein et al., 2015). It should be noted that steppic vegetation with herbaceous communities existed during glacial periods (Bottema, 1995; Wick et al., 2003; Messager et al., 2013; Pickarski et al., 2015). This may be the reason for the relatively limited sediment removal (by erosion) that is characteristic of lithofacies 2.

Impact of Mediterranean warm climatic conditions on cyclic fluvial evolution

By analogy with the evolution during the formation of T16, it may be inferred that the Göksu River completed its terrace aggradation process during a single climatic cycle embracing both a warm and a cold period (MIS 7 and 6). The river incised its valley during the previous (MIS 8 to 7) and next (MIS 6 to 5) cold-to-warm transitions, although a small patch of MIS 5 deposits was laid down at the top of the terrace sequence before the incision. The fluvial sedimentary succession of interglacial deposits (as during MIS 7) overlain by glacial ones (as during MIS 6) resembles one that is often present in cold-temperate conditions, such as in river terraces in the English Midlands (Gibbard and Lewin, 2009; Maddy and Bridgland, 2000; Maddy et al., 2001). This succession is represented as the second scenario of fluvial terrace development in temperate to periglacial conditions proposed by Vandenberghe (2015). In that scenario, interglacial fluvial deposits (MIS 7) were not completely removed by the river at the beginning of the next cold period (MIS 6).

However, there are also some obvious differences with the common fluvial successions in the cool-temperate regions. First, most striking in the Göksu River is the generally gradual transition between the two styles (facies) of fluvial deposition, corresponding to the transition between interglacial and glacial deposition, without a distinct erosive boundary. This pattern is in contrast to the alternating temperate–cold conditions, for which a distinct erosion phase is generally registered between the warm and the cold periods (Mol et al., 2000). The two lithofacies types in the Göksu River may represent continuous, internal evolution from a high-energy channel (in the warm period) to high-stage flood deposition (in the cold period). Second, the interglacial deposits of the Göksu River contain coarse-grained and inorganic sediments. This also contrasts with the generally observed fine-grained, meandering river types that are characteristic of warm periods in temperate to cold environments (e.g., Vandenberghe, 2001).

Furthermore, some other studies from temperate environments invoke a range of different climatic conditions during interglaciations to explain depositional river activity. For instance, in the Pyrenees foreland, Stange et al. (2013) related aggradation during interglaciations to (short) stadial episodes. In contrast, Olszak (2011) and Olszak et al. (2016) explained terrace accumulations during MIS 5 and 3 in the west Carpathians as due to aggradation during interstades or interglaciations.

The morphological expression of the fluvial processes is evidently governed by the balance between discharge and sediment load of the river. These two variables are a function of climate and vegetation cover, which in the Mediterranean environment may be quite different from the cool-temperate environment. Without considering variability in precipitation, for which we have no information, an attempt is made to explain the differences in fluvial development between the two environmental systems. A main point is the vegetation cover, as it is very influential in controlling supply of sediment to the river (Vandenberghe, 1993, 1995, 2001). In general, incision during climatic transitions in temperate conditions appears to be caused by decreased sediment availability as a result of delayed response of vegetation growth or decline with respect to climatic change (Vandenberghe, 1995). However, according to Şenkul and Doğan (2013), vegetation cover occupied 80–90% of the surface of northwestern Anatolia and the Black Sea coast, and 50–60%

along the Mediterranean coast during the last glacial period. Only between ~18 and 16 ka did a brief interval of cold and arid conditions result in weaker steppe vegetation over some parts of Anatolia (Şenkul and Doğan, 2013). Similarly, according to the detailed analyses of the Van Lake pollen, xerophytic steppe vegetation was dominant in eastern Anatolia during MIS 2, and there were rapid expansions and contractions of tree populations that reflect variability in temperature and moisture availability. (Pickarski et al., 2015).

Cold periods were possibly less severe at moderate altitudes (0–500 m above sea level for the Göksu River in south Anatolia) than in other cooler environments and may have been associated with a steppic vegetation cover. Thus, it is suggested that in Anatolia, the continuously present steppic vegetation during cold periods may have maintained similar sedimentary processes and river patterns as during the preceding more densely vegetated interglacial period. The fining upward trend of the fluvial sediment may have been the result of internal dynamics, wherein the continuing aggradation caused the floodplain to gradually become higher in position, and the coarsest gravel could finally no longer reach the floodplain (such as in the deposits of T16).

Similarly, the absence of a clear erosional event at the warm-to-cold transition may also be attributed to the weak change in vegetation cover resulting in only a slight decrease in evapotranspiration and thus only slightly increased runoff. A relatively less severe climate during the cold period compared with northern and central Europe could also have had a different effect: there are no indications in lowland Anatolia for long-lasting winter frost or permafrost that would have increased peak surface runoff. Thus, the weak changes of vegetation cover in comparison with cooler temperate regions and the absence of seasonal or perennial frozen ground would have prevented an erosional effect at the warm–cold transition.

In contrast, the prominent risers between the different river terrace levels demonstrate that there were distinct incision phases. This is not surprising, if we take into account the continuous relative uplift of the Göksu catchment during the Quaternary (after the formation of T16, the river has incised about 12 m in the past ca. 200 ka). By analogy with the depositional sequence within T16 embracing an interglacial–glacial cycle, we hypothesize that the erosional steps in the terrace staircase took place mainly at the cold-to-warm transitions (in the case of T16, from MIS 8 to 7 and from MIS 6 to 5). In the temperate regions, increased slope stability due to delayed vegetation response to the climatic change has been considered responsible for distinct erosion at such cold-to-warm transitions (Vandenberghe, 1995). However, if the Mediterranean regions were characterized by weak changes in vegetation cover at climatic transitions, there must be another reason for the initiation of erosion in those regions. As in cooler temperate regions, precipitation may have increased during the transition to an interglacial climate. Although warm periods may not have been affected by intense periglacial conditions, it is quite possible, especially at the beginning of warm periods, that precipitation was in the form of snow, and a thick snow cover may have been present during winter. Rapid thaw in spring would have resulted in considerable runoff, and thus erosion, at the cold-to-warm transition. Such an explanation was invoked by Doğan (2011), who reported high discharge after strong snow melting over frozen soils at the beginning of a warm period in the Kızılırmak River in Anatolia. Doğan (2011) suggested that snow accumulation occurred consistently during the entire interglacial period in the Anatolian mountains, keeping discharges high. Similar explanations could apply to interglacial fluvial action in other hilly (or mountainous) regions (von Suchodoletz et al., 2015). As a conclusion, we agree with Doğan (2011) and von Suchodoletz et al. (2015) that local or regional influences, such as specific tectonic movements, soil frost, and vegetation cover, should not be neglected in explaining fluvial evolution.

CONCLUSIONS

The Göksu River, located in the Taurus orogenic zone and the warm continental Mediterranean climatic region, appears to have responded to tectonic and climatic factors. Even though the uplift seems to have created 16 river terrace levels, the successive accumulation and incision features of the river point to climatic cyclicity. Evidence from OSL dating of the youngest river terrace indicates that the Göksu River deposited its sediments under different climatic conditions. Two phases of deposition are represented by lithofacies 1 and 2 that correspond with MIS 7 and 6. Correlation of the OSL-dated sediments with global marine ^{18}O curves indicates that fluvial accumulation started in an interglacial period and continued during the next glacial period, with incision presumed at the cold–warm transition at the beginning of the cycle. According to our ages, it is striking that the fluvial morphologic (wandering system) and sedimentologic styles (lithofacies 1 and 2) between glacial and interglacial periods were not very different and that fluvial erosion was not well pronounced at the warm-to-cold transition. Although the fluvial cyclicity in both cold-temperate and Mediterranean conditions appears to be strongly influenced by vegetation cover, the Mediterranean lowlands were probably characterized by only weak differences in vegetation cover between glacial and interglacial times. This resulted in modest erosional activity at the warm-to-cold transition, in contrast to cool/temperate regions. Initiation of the incision of the river terrace levels at the cold-to-warm transition is hypothetically attributed to the impact of the thaw of large amounts of snow at the beginning of climatic warming. In general, it may be confirmed from this study that local conditions may significantly influence fluvial evolution.

ACKNOWLEDGMENTS

by David Bridgland and an anonymous reviewer are also gratefully acknowledged. We are very grateful for support and suggestions from the editors, Lewis Owen and Becky Briant, which improved the article substantially.

REFERENCES

Akarsu, İ.,1960. *The Geology around Mut. MTA Report No. 2444*. Ankara, Turkey.

Avşin, N., 2011.The role of climate and tectonic on formation of Kızılırmak River terrace, Avanos. *Turkish Journal of Geographical Sciences* 9, 221–238.

Bassant, P., Buchem, V., Strasser, A., Görür, N., 2005. The stratigraphic architecture and evolution of the Burdigalian carbonate–siliciclastic sedimentary systems of the Mut Basin, Turkey. *Sedimentary Geology* 173, 187–232.

Bottema, S., 1995. The Younger Dryas in the Eastern Mediterranean. *Quaternary Science Reviews* 14, 883–891.

Bøtter-Jensen, L. 1997. Luminescence techniques: instrumentation and methods. *Radiation Measurements* 17, 749–768.

Bridge, J., 2003. *Rivers and Floodplains. Forms, Processes and Sedimentary Record*. Blackwell publishing, USA

Bridgland, D., 2000. River terrace systems in northwest Europe: an archive of environmental change, uplift and early human occupation. *Quaternary Science Reviews* 19, 1293–1303.

Bridgland, D., Allen, P., 1996. A revised model for terrace formation and its significance for the lower Middle Pleistocene Thames terrace aggradations of northeast Essex, UK. In: Turner, C. (Ed.), *The Early Middle Pleistocene in Europe*. Balkema, Rotterdam, pp. 121–134.

Bridgland, D., Demir, T., Seyrek, A., Daoud, M., Abou Romieh, M., Westaway, R., 2017. River terrace development in the NE Mediterranean region (Syria and Turkey): patterns in relation to crustal type. *Quaternary Science Reviews* 166, 307–323.

Büdel, J., 1977. *Klima-Geomorphologie*. Gebrüder Borntraeger, Berlin.

Carson, M.A., 1984. Observations on the meandering-braided river transition, the Canterbury plains, New Zealand, Part 2. *New Zealand Geographer* 40(2), 89–99.

Church, M., 1983. Pattern of instability in a wandering gravel bed channel. In: Collinson, J.D., Lewin, J. (Eds.), *Modern and Ancient Fluvial Systems*. International Association of Sedimentologists, Blackwell Scientific, Oxford, UK, pp. 169–180.

Çiçek, İ., 2001. The geomorphology of Mut around Fırat University. *Journal of Social Sciences* 11, 1–20.

Cohen, K.M., Gibbard, P.L., 2011. *Global Chronostratigraphical Correlation Table for the Last 2.7 Million Years*. Subcommission on Quaternary Stratigraphy, International Commission on Stratigraphy, Cambridge, UK.

Cordier, T., Robin, C., Capdevielle, X., Fabreguettes, O., Desprez-Loustau, M., Vacher, C., 2012. The composition of phyllosphere fungal assemblages of European beech (*Fagus sylvatica*) varies significantly along an elevation gradient. *New Phytologist* 196, 510–519.

Demir, T., Seyrek, A., Westaway, R., Guillou, H., Scaillet, S., Beck, A., 2012. Late Cenozoic regional uplift and localised crustal deformation within the northern Arabian Platform in southeast Turkey: Investigation of the Euphrates terrace staircase using multidisciplinary techniques", *Geomorphology*, 165, 7–24

Doğan, U., 2010. Fluvial response to climate change during and after the Last Glacial Maximum in Central Anatolia, Turkey. *Quaternary International* 222, 221–229.

Doğan, U., 2011. Climate-controlled river terrace formation in the Kızılırmak Valley, Cappadocia section, Turkey: inferred from Ar–Ar dating of Quaternary basalts and terraces stratigraphy. *Geomorphology* 126, 66–81.

Eriş, K., Bassant, P., Ülgen, B., 2005. Tectono-stratigraphic evolution of an Early Miocene incised valley-fill (Derincay Formation) in the Mut Basin, Southern Turkey. *Sedimentary Geology* 173, 151–185.

Gedik, K., Yılmaz, H., Yoldaş, R., 1979. *The Geology and Petrol Possibility of Mut, Ermenek and Silifke Region.TJK Bulletin C22*. Ankara, Turkey.

Görür, N., Oktay, F.Y., Seymen, I., and Şengör, A.M.C., 1984, Paleotectonic evolution of the Tuzgölü basin complex, central Turkey: sedimentary record of a Neotethyan closure. In: Dixon, J.E., Robertson, A.H.F. (Eds.), *The Geological Evolution of the Eastern Mediterranean. Geological Society of London Special Publication* 17, 467–482.

Maddy, D., Bridgland, D., 2000. Accelerated uplift resulting from Anglian glacioisostatic rebound in the Middle Thames Valley, UK?: Evidence from the river terrace record. *Quaternary Science Reviews* 19, 1581–1588

Maddy, D., Bridgland, D., Westaway, R. 2001. Uplift-driven valley incision and climate-controlled river terrace development in the Thames Valley, UK. *Quaternary International* 79, 23–36.

Maddy, D., Demir, T., Bridgland, D., Veldkamp, A., Stemerdink, C., van der Schriek, T., Westaway, R., 2005. An obliquity-controlled Early Pleistocene river terrace record from Western Turkey. *Quaternary Research* 63, 339–346.

Maddy, D., Demir, T., Bridgland, D., Veldkamp, A., Stemerdink, C., van der Schriek, T., Schreve, D., 2008. The Pliocene initiation and Early Pleistocene volcanic disruption of the paleo-Gediz fluvial system, Western Turkey. *Quaternary Science Reviews* 26, 2864–2882.

Makaske, B., 2001. Anastomosing rivers: a review of their classification, origin and sedimentary products. *Earth-Science Reviews* 53, 149–96.

Map General Command (HGK), 2000. 1:25,000 topographic maps. Ankara.

Messager, E., Belmecheri, S., Von Grafenstein, U., Nomade, S., Ollivier, V., Voinchet, P., Puaud, S., *et al*., 2013. Late Quaternary record of the vegetation and catchment-related changes from Lake Paravani (Javakheti, South Caucasus). *Quaternary Science Reviews* 77, 125–140.

Miall, A., 1996. *The Geology of Fluvial Deposits*. Springer, Berlin.

Mine Technical Search Institude (MTA), 1996. 1:25,000 geologic maps. Ankara.

Mol, J., Vandenberghe, J., Kasse, C. 2000 River response to variations of periglacial climate. *Geomorphology* 33, 131–148.

Murray, A., Wintle, A., 2000. Luminescence dating of quartz using an improved single-aliquot regenerative-dose protocol. *Radiation Measurements* 32, 57–73.

Olley, J.M., Murray, A.S., Roberts, R.G., 1996. The effects of disequilibria in the uranium and thorium decay chains on burial dose rates in fluvial sediments. *Quaternary Geochronology* 15, 751–760.

Olszak, J. M., 2011. Evolution of fluvial terraces in response to climate change and tectonic uplift during the Pleistocene: Evidence from Kamienica and Ochotnica River valleys (Polish Outer Carpathians). *Geomorphology*, 129: 71–78.

Olszak, J., Adamiec, G., 2016. OSL-based chronostratigraphy of river terraces in mountainous areas, Dunajec basin, West Carpathians: a revision of the climatostratigraphical approach. *Boreas* 45, 483–493.

Öğretmen, N., Cipollari, P., Frezza, V., Faranda, C., Karanika, K., Gliozzi, E., Radeff, G., Cosentino, D., 2018. Evidence for 1.5 km of uplift of the central Anatolian Plateau's southern margin in the last 450 kyr and Implications for Its Multiphased Uplift History. *Tectonics* 37, 359–390.

Penck, A., Bruckner, E., 1909. *Die Alpen im Eiszeitalter*. Leipzig. 1199 pp.

Peters, G., Van Balen, R.T., 2007. Pleistocene tectonics inferred from the fluvial terraces of the northern Upper Rhine Graben, Germany. *Tectonophysics* 430, 41–65.

Pickarski, N., Kwiecien, O., Langgut, D., Litt, T., 2015. Abrupt climate and vegetation variability of eastern Anatolia during the last glacial. *Climate of the Past* 11, 1491–1505.

Prescott, J.R., Hutton, J.T., 1988. Cosmic ray and gamma ray dosimetry for TL and ESR. *Nuclear Tracks and Radiation Measurements* 14, 223–227.

Schielein, P., Schellmann, G., Lomax, J., Preusser, F., Fiebig, M., 2015. Chronostratigraphy of the Hochterassen in the lower Lech valley (North Alpine Foreland). *Quaternary Science Journal* 64(1), 15–29.

Schildgen, T., Cosentino, D., Bookhagen, B., Niedermann, S., Yıldırım, C., Echtler, H., Wittman, H., Strecker, M., 2012. Multiphased uplift of the southern margin of the Central Anatolian plateau, Turkey: a record of tectonic and upper mantle processes. *Earth and Planetary Science Letters* 317, 85–95.

Schumm, S., 1977. *The Fluvial System*. Wiley, New York.

Schumm, S., 1981. Evolution and response of the fluvial system: sedimentologic implications. *Society of Economic Paleontologists and Mineralogists, Special Publication* 31, 19–29.

Şengör, C., Yılmaz, Y. 1981. Tethyan evolution of Turkey: a plate tectonic approach. *Tectonophysics* 75, 181–241.

Şenkul, Ç., Doğan, U., 2013. Vegetation and climate of Anatolia and adjacent regions during the Last Glacial period. *Quaternary International* 302, 110–122.

Stange, K., Van Balen, R.T., Carcaillet, J., Vandenberghe, J., 2013. Terrace staircase development in the Southern Pyrenees Foreland: inferences from 10Be terrace exposure ages at the Segre River. *Global and Planetary Change* 101, 97–112.

Starkel, L., 2003. Climatically controlled terraces in uplifting mountain areas. *Quaternary Science Reviews* 22, 2189–2198.

Starkel, L., Michczynska, D., Gebica, P., Kiss, T., Panin, A., 2015. Climatic fluctuations reflected in the evolution of fluvial systems of Central–Eastern Europe (60–8 ka cal BP). *Quaternary International* 388, 97–118.

Tanar, Ü., 1989, Gökçen, N., 1990. *Stratigraphy and Micropaleontology of Mut-Ermenek Tertiary Stack. MTA Bulletin S.* 110. Ankara, Turkey.

Tebbens, L., Veldkamp, A., 2001. Exploring the possibilities and limitations of modelling Quaternary fluvial dynamics. In: Maddy, D., Macklin, M., Woodward, J. (Eds.), *River Basin Sediment Systems: Archives of Environmental Change*. Balkema, Rotterdam, pp. 469–484.

Vandenberghe, J., 1993. Changing fluvial processes under changing periglacial conditions. *Supplemental Band* Zeitschrift für Geomorphologie 88, 17–28.

Vandenberghe, J., 1995. Timescales, climate and river development. *Quaternary Science Reviews* 14, 631–638.

Vandenberghe, J., 2001. A typology of Pleistocene cold-based rivers. *Quaternary International* 79, 111–121.

Vandenberghe, J., 2002. The relation between climate and river processes, landforms and deposits during the Quaternary. *Quaternary International* 91, 17–23.

Vandenberghe, J., 2008. The fluvial cycle at cold-warm-cold transitions in lowland regions: a refinement of theory. *Geomorphology* 98, 275–284.

Vandenberghe, J., 2015. River terraces as a response to climatic forcing: formation processes, sedimentary characteristics and sites for human occupation. *Earth and Climate*, 370, 3–11.

Vandenberghe, J., Maddy, D., 2001. Response of river systems to climate change. *Quaternary International* 79, 1–3.

Vandenberghe, J., Wang, X., Lu, H., 2011. Differential impact of small-scaled tectonic movements on fluvial morphology and sedimentology (the Huang Shui catchment, NE Tibet Plateau). *Geomorphology* 134, 171–185.

Wang, X., Vandenberghe, J., Shuangwen, Y., Van Balen, R.T., Lu, H., 2015. Climate-dependent fluvial architecture and processes on a suborbital timescale in areas of rapid tectonic uplift: an example from the NE Tibetan Plateau. *Global and Planetary Change* 133, 318–329.

Westaway, R., Guillou, H., Yurtmen, S., Beck, A., Bridgland, D., Demir, T., Scaillet, S., Rowbotham, G., 2006. Late Cenozoic uplift of western Turkey: improved dating of the Kula Quaternary volcanic field and numerical modelling of the Gediz River terrace staircase. *Global and Planetary Change* 51, 131–171.

Westaway, R., Pringle, M., Yurtmen, S., Demir, T., Bridgland, D., Rowbotham, G., Maddy, D., 2004. Pliocene and Quaternary regional uplift in western Turkey: the Gediz River terrace staircase and the volcanism at Kula. *Tectonophysics* 391, 121–169.

Wick, L., Lemcke, G., Sturm, M., 2003. Evidence of Lateglacial and Holocene climatic change and human impact in eastern Anatolia: high resolution pollen, charcoal, isotopic and geochemical records from the laminated sediments of Van Lake, Turkey. *The Holocene* 13, 665–675.

von Suchodoletz, H., Gärtner, A., Hoth, S., Umlauft, J., Sukhishvili, L., Faust, D., 2016. Late Pleistocene river migrations in response to thrust belt advance and sediment-flux steering—the Kura River (southern Caucasus). *Geomorphology* 266, 53–65.

von Suchodoletz, H., Menz, M., Kühn, P., Sukhishvili, L., Faust, D., 2015. Fluvial sediments of the Algeti River in southeastern Georgia—an archive of Late Quaternary landscape activity and stability in the Transcaucasian region. *Catena* 130, 95–107.

Gibbard, L., Lewin, C., 2009. River incision and terrace formation in the Late Cenozoic of Europe. *Tectonophysics* 474, 41–55.